Original Article

MOLECULAR METABOLISM

Zmiz1 is required for mature β-cell function and mass expansion upon high fat feeding

Tamadher A. Alghamdi [1], Nicole A.J. Krentz [2], Nancy Smith [1], Aliya F. Spigelman [1], Varsha Rajesh [2], Alokkumar Jha [2], Mourad Ferdaoussi [3], Kunimasa Suzuki [1], Jing Yang [2], Jocelyn E. Manning Fox [1], Han Sun [2], Zijie Sun [4], Anna L. Gloyn [2,5,6,**], Patrick E. MacDonald [1,*]

ABSTRACT

Objective: Identifying the transcripts which mediate genetic association signals for type 2 diabetes (T2D) is critical to understand disease mechanisms. Studies in pancreatic islets support the transcription factor *ZMIZ1* as a transcript underlying a T2D GWAS signal, but how it influences T2D risk is unknown.

Methods: β-Cell-specific *Zmiz1* knockout ($Zmiz1^{\beta KO}$) mice were generated and phenotypically characterised. Glucose homeostasis was assessed in $Zmiz1^{\beta KO}$ mice and their control littermates on chow diet (CD) and high fat diet (HFD). Islet morphology and function were examined by immunohistochemistry and *in vitro* islet function was assessed by dynamic insulin secretion assay. Transcript and protein expression were assessed by RNA sequencing and Western blotting. In islets isolated from genotyped human donors, we assessed glucose-dependent insulin secretion and islet insulin content by static incubation assay.

Results: Male and female $Zmiz1^{\beta KO}$ mice were glucose intolerant with impaired insulin secretion, compared with control littermates. Transcriptomic profiling of $Zmiz1^{\beta KO}$ islets identified over 500 differentially expressed genes including those involved in β-cell function and maturity, which we confirmed at the protein level. Upon HFD, $Zmiz1^{\beta KO}$ mice fail to expand β-cell mass and become severely diabetic. Human islets from carriers of the *ZMIZ1*-linked T2D-risk alleles have reduced islet insulin content and glucose-stimulated insulin secretion.

Conclusions: β-Cell Zmiz1 is required for normal glucose homeostasis. Genetic variation at the *ZMIZ1* locus may influence T2D-risk by reducing islet mass expansion upon metabolic stress and the ability to maintain a mature β-cell state.

Keywords Islets of langerhans; Insulin; Secretion; Diabetes

1. INTRODUCTION

Despite considerable progress in uncovering the genetic landscape for type 2 diabetes (T2D), progress in moving from a genetic association signal to effector transcripts and downstream biology remains slow [1]. Most genetic signals associated with T2D risk are located in non-coding regions, suggesting that they likely confer their risk through effects on gene expression [2–4]. We previously used expression quantitative trait locus (eQTL) analyses to identify T2D-risk variants, which also alter transcript expression in human islets, and identified *ZMIZ1* as the likely effector transcript at a locus on chromosome 10 [5].

ZMIZ1 (Zinc Finger MIZ-Type Containing 1) was first identified as a co-activator of the androgen receptor in human prostate epithelial cells [6] and is a member of the Protein Inhibitor of Activated STAT (PIAS)-like family, a group of proteins that regulate transcription through several mechanisms including blocking DNA-binding of transcription factors, recruiting transcriptional coactivators or corepressors, and protein SUMOylation [7]. ZMIZ1 regulates several transcription factors including p53 [8], Smad3 [9], and Notch1 [10]. Complete deletion of *Zmiz1* in mice is embryonically lethal due to impaired vascular development [11]. In humans, we previously identified *ZMIZ1* as a causal transcript associated with T2D risk [5]. We showed that overexpression of *ZMIZ1* reduced glucose-stimulated insulin-secretion whilst knockdown of *ZMIZ1* inhibited KCl-induced secretion in primary human islets [5]. Separately, knockdown of *ZMIZ1* in the human β-cell line EndoC-βH1 resulted in reduced insulin secretion and cell count

[1]Department of Pharmacology and Alberta Diabetes Institute, University of Alberta, Edmonton, AB, T6G2R3, Canada [2]Division of Endocrinology, Department of Pediatrics, Stanford University School of Medicine, Stanford, CA, USA [3]Department of Pediatrics, University of Alberta, Edmonton AB, T6G2R3, Canada [4]Beckman Research Institute, City of Hope, Duarte, CA, USA [5]Stanford Diabetes Research Centre, Stanford University, Stanford, CA, USA [6]Oxford Centre for Diabetes Endocrinology & Metabolism, Radcliffe Department of Medicine, University of Oxford, UK

*Corresponding author. Alberta Diabetes Institute, LKS Centre, Rm. 6-126, Edmonton, AB, T6G 2R3, Canada. E-mail: pmacdonald@ualberta.ca (P.E. MacDonald).

**Corresponding author. Center for Academic Medicine, Division of Endocrinology & Diabetes, Department of Pediatrics, 453 Quarry Road, Palo Alto CA, 94304, USA. E-mail: agloyn@stanford.edu (A.L. Gloyn).

URL: http://www.bcell.org

Received July 25, 2022 • Revision received October 15, 2022 • Accepted October 19, 2022 • Available online 26 October 2022

https://doi.org/10.1016/j.molmet.2022.101621

[12]. How altered *ZMIZ1* expression contributes to T2D risk and influences insulin secretion remain poorly understood.

In the current study, we characterised male and female mice bearing *Zmiz1* null β-cells and investigated the impact of T2D-associated variants at the *ZMIZ1* locus on β-cell function in islets from carriers without diabetes. In mice, we demonstrate a role for Zmiz1 in maintaining β-cell maturation, function, and expansion upon metabolic stress. In human islets, we show an association of *ZMIZ1* T2D-risk alleles with reduced insulin content and glucose stimulated insulin secretion.

2. METHODS

2.1. Animal studies

ROSA26 Cre reporter (also known as R26R) mice [B6; 129S4-*Gt(ROSA)26Sor*^{tm1Sor}/J] [13] were obtained from the Jackson Laboratory (Bar Harbor, ME). Ins1-Cre knock-in mice [14] were kept on a C57Bl/6J genetic background. *Zmiz1*$^{fl/fl}$ mice were generated by flanking coding exons 8 to 11 (149–416 amino acids) of *Zmiz1* with two loxP sequences that also introduced a frame shift after exon 11 resulting in no detectable protein production using antibodies directed towards both the N- and C-termini (not shown). *Zmiz1*$^{fl/fl}$ mice were maintained on a C57Bl/6J genetic background. Ins1-Cre knock-in mice were crossed with *Zmiz1*$^{fl/fl}$ mice to generate the following cohorts of male and female mice: *Ins1-Cre*$^{+}$ *Zmiz1*$^{+/+}$, *Ins1-Cre*$^{+}$ *Zmiz1*$^{fl/+}$, and *Ins1-Cre*$^{+}$ *Zmiz1*$^{fl/fl}$; referred to as Zmiz1^{Ctrl}, Zmiz1$^{\beta HET}$, and Zmiz1$^{\beta KO}$, respectively. Mice were fed chow diet (5L0D*, PicoLab Laboratory Rodent Diet) until 12 weeks of age, after which time some mice were switched to high fat diet (HFD; 60% fat; Bio-Serv, CA89067-471) for an additional 8 weeks.

Mice were fasted for 4–6 h and had access to water prior to oral glucose tolerance test (OGTT) (1 g/kg dextrose) [15] or intraperitoneal glucose tolerance test (IPGTT) (1 g/kg dextrose) [16] for chow fed groups (12 weeks of age). For HFD groups, 0.5 g/kg dextrose was used for both OGTT and IPGTT (20 weeks of age). Blood was collected every 15 min for 2 h and centrifuged at 4 °C for 10 min at 10,000 rpm. Glucose levels were measured using One Touch Ultra 2 glucometer (LifeScan Canada Ltd.; Burnaby, British Columbia, Canada), and plasma insulin levels were assessed using Insulin Rodent (Mouse/Rat) Chemiluminescence ELISA (cat# 80-INSMR-CH01, CH10, ALPCO, NH, USA). Insulin tolerance tests (ITTs) [17] were performed by intraperitoneal injection of insulin 1 U/kg Humulin R (Eli Lilly) and blood glucose levels were assessed after the initial insulin delivery every 15 min for 2 h.

For islet isolation and perifusion, pancreas of euthanized mice were perfused with collagenase [18]. Isolated islets were hand-picked or subjected to purification using Histopaque Gradient Centrifugation [19] and were cultured overnight. Glucose-stimulated insulin secretion was determined as previously described [20].

2.2. β-Galactosidase expression

Enzymatic X-gal staining of pancreas cryosections (5 μm thickness) was performed using an X-Gal Staining Kit (Cat#GX10003, Oz Biosciences INC, San Diego, CA, US) according to the manufacturer's instructions. Briefly, cryosections were thawed and washed with 1× PBS. Sections were fixed with fixing buffer for 15 min at room temperature and then washed 2 times with 1× PBS. Freshly prepared 1× staining solution of X-Gal (5-bromo-4chloro-3-indoyl-β-D-galactopyranoside) was added to each section and incubated in a humidified environment at 37 °C overnight. The following day, slides were washed once with 1× PBS. ProLong Gold anti-fade reagent (P36930, Invitrogen) was applied, and slides were allowed to dry. Pancreatic sections were imaged under bright-field with an Olympus DP27 micrscope.

2.3. Immunohistochemistry and β cell mass assessment

Mouse pancreas was weighed before fixing in Z-fix (VWR) and embedded with paraffin. Paraffin-embedded pancreatic tissue sections (3 μm thickness separated by 200 μm) were rehydrated and subjected to antigen retrieval with sodium citrate buffer (10 mM Sodium citrate, 0.05% tween 20, pH 6.0) microwaved for 15 min at high temperature and allowed to cool for 20–40 min. 0.1% Triton-X (T9284, Sigma) was added for permeabilization for 5 min and slides were washed with 1× PBS 3 times for 5 min each. Tissues sections were then blocked with 20% goat serum (G9023, Sigma) for 30 min and stained with insulin antibody (dilution 1:5, IR002, Dako) for 1 h at room temperature and washed 3 times with 1× PBS. Tissue sections were incubated with Alexa Fluor 488 goat anti-guinea pig (dilution 1:200, A11073, Invitrogen) secondary antibody for 1 h at room temperature. Slides were then washed with 1× PBS 3 times and ProLong Gold anti-fade reagent with DAPI (P36931, Invitrogen) was applied. Slides were allowed to dry before imaging. Pancreatic sections were imaged at 10× objective using Zeiss COLIBRI Fluorescence Microscope and LED light source with 350-, 495-, or 555-nm filter set. For each animal, 3–4 sections were analyzed. Insulin-positive area was quantified with ImageJ software (NIH Image). The β cell mass was determined as the relative insulin-positive area of each section normalized to pancreas weight.

2.4. RNA extraction, sequencing, and quantification

150 islets from chow-fed female Zmiz1^{Ctrl} (n = 3), female Zmiz1$^{\beta 1KO}$ (n = 4), male Zmiz1^{Ctrl} (n = 4), and male Zmiz1$^{\beta 1KO}$ (n = 3) mice were lysed in 1 mL of TRIzol Reagent (ThermoFisher Scientific) for RNA extraction as per manufacturer instructions. Library preparation and sequencing was performed by the Oxford Genomic Centre (Wellcome Centre for Human Genetics, Oxford, UK). All libraries were multiplexed and sequenced as 100-nucleotide paired-end reads. RNA libraries were sequenced to a mean depth of 32 (±1.7) million reads per sample. STAR v2.5 [21] was used to map reads to the mouse genome build GRCm38 with GENCODE m23 as the transcriptome reference. To quantify gene-level counts, featureCounts from the Subread package v1.5 was used (http://subread.sourceforge.net/) [22].

2.5. PCA and differential expression analysis

Genes detected in all 14 samples at >1 count per million (cpm) were retained for downstream analysis, resulting in 12,047 protein-coding genes. Counts were normalised and transformed to log-cpm using the *voom* function within the *limma* package (v.3.32.5) [23] in R (v.3.3.2). Batch effect of islet isolations was corrected using *removeBatchEffect* in *limma* before principal component analysis. DESeq2 (v1.26.0) [24] was used to identify 556 differentially-expressed genes (padj < 0.05) between control and knockout islets. The online tool Integrated System for Motif Activity Response Analysis (ISMARA) was used for computationally predicted regulatory sites for transcription factors (https://ismara.unibas.ch/mara/) [25].

2.6. Real time PCR

RNA was extracted with TRIzol (Thermo Fisher) and 100 ng was reverse-transcribed using a One script Plus cDNA synthesis kit (Applied Biological Materials Inc.). For the quantification of N-terminal or C-terminal *Zmiz1* transcript, the following primers were used: for N-terminal (forward 5′-CCTAGCAGGAGGATGGACCTTGAGTGAAG-3′/reverse 5′-GGTTCTGTAAGTGCTGCTTGA-TGCACTGC-3′), and for C-terminal (forward 5′-GCATGTGCAGTGCTTTGACCTGGAGTC-3′/reverse 5′-GGAGTGTTGGATGGCGTTCAGGATC-3′). The qPCR was carried out

using a PowerUp SYBR Green Master mix and an Applied Biosystems StepOne Plus Real-Time PCR system (Thermo Fisher): 10 min at 95 °C, 40 cycles of 30s at 95 °C, and then 1 min at 60 °C.

2.7. Western blotting

Isolated islets were cultured overnight in RPMI with 11.1 mM glucose. Islets (n = 100–200) were picked, washed once with 1× Dulbecco's Phosphate Buffered Saline (14190-144; gibco) PBS, and collected in 30 μl of cell lysis buffer (C2978, Sigma) supplemented with protease inhibitor cocktail (P8340, Sigma). Islets were sonicated by using Heat Systems-Ultrasonics W-385 Sonicator Ultrasonic Processor at 4 °C. Protein concentration was estimated by Quick Start Bradford 1 × Dye reagent (5000205, BioRad) using a microplate reader (EnVision Multilabel Plate Reader, PerkinElmer). A non-reducing lane marker sample buffer (39001, Thermo Scientific) was added to a total of 5 or 10 μg of protein from islet cell lysates and the mixture was heated for 5 min at 95 °C. Samples were then loaded, separated by SDS-PAGE (7.5% or 10% gel), and transferred to PVDF Immobilon-P transfer membrane (IPVH00010, Millipore). Membranes were blocked by 5% milk in Tris-buffered saline with 0.1% tween 20 (TBST) for 1 h at room temperature, then probed with primary antibodies in 5% bovine serum albumin (BSA) in TBST overnight at 4 °C with the following concentrations: Zmiz1 (1:1000, Santa Cruz sc-376825), CD81 (dilution 1:1000; Cell Signaling 10037S), Aldh1a3 (dilution 1:1000, Novus biologicals NBP2-15339), β-actin (dilution 1:2000; Santa Cruz sc-47778), Notch1 (dilution 1:200, Novus biologicals NB100-78486SS), c-Myc (dilution 1:200, Novus biologicals NB200-108SS), Ki67 (dilution 1:200, Novus biologicals NB500-170SS). The following day, membranes were washed three times with 1× TBST and incubated with secondary antibodies in 5% milk in TBST for 1 h at room temperature with the following concentration of secondary antibodies, conjugated with horseradish peroxidase: donkey anti-rabbit IgG (1:5000, NA934, GE Healthcare), goat anti-rabbit IgG (1:5000, 111-035-144, Jackson ImmunoResearch) and goat anti-mouse IgG (1:5000, 115-035-146, Jackson ImmunoResearch). Membranes were washed three times with 1× TBST and incubated with ECL (45002401, GE Healthcare) for 5 min. Protein bands were imaged by ChemiDoc imaging system (Bio-Rad).

2.8. Luciferase assay

Luciferase reporter assays were performed by cloning the 150-bp regions surrounding rs703972 and rs12571751 into pGL3-Promoter [luc+] Firefly Luciferase vector (E1761; Promega, Madison, WI). PCR primers were used to amplify the rs703972 region (5′-CTCCTACTGTCCTTGCTTCAC-3′ and 5′-ACTGATGACTTCCTCACCTTAAA-3′) and rs12571751 region (5′-GGGTCTCCATGGCGATTAAA-3′ and 5′-CACCATACTAACTGCCCTACTC-3′). The PCR products were cloned into the pGL3-Promoter plasmid in both the forward and reverse direction using the KpnI and XhoI restriction enzymes. DNA for human islet donor R331 and R339 was used to PCR the rs12571751A allele/rs703972G allele and rs12571751G allele/rs703972C allele, respectively. Human EndoC-βH1 cells [58] were transfected with 500 ng of empty pGL3-Promoter vector or pGL3-Zmiz1 vectors with FuGENE 6 transfection reagent (Fisher Scientific) and cotransfected with 10 ng of pGL4.74 [hRluc/TK] Renilla Luciferase vector (Promega) using a FuGENE:DNA ratio of 6:1. Dual-Luciferase Reporter Assay kit (Promega) was used to measure luciferase activities 48 h after transfection and firefly luciferase activity was normalized to the Renilla luciferase activity.

2.9. Human islet studies

Isolation of human islets and static glucose-stimulated insulin secretion assay have been described in the protocols.io repository [26]. Insulin was assayed by chemiluminescence (cat# 80-INSHU-CH01, ALPCO) that detects human insulin with no cross-reactivity to mouse or rat insulin, the major human proinsulin form (des (31, 32)), or either human or rodent c-peptide. DNA was extracted from exocrine tissue, spleen, or, if no other tissue was available, islets. Genotyping was performed on Illumina Omni2.5Exome-8 version 1.3 BeadChip array. Allelic imbalance was performed on ATAC-seq of 17 islets [27] that were processed following the ENCODE ATAC-Seq pipeline (v1.9.3). Overlapping reads with the 10 SNPs in the 99% credible set [28] were remapped by WASP (v0.3.4) to correct mapping bias. SNPs and samples were further filtered based on the parameters (read depth ≥ 5 for each allele and heterozygous samples > 2) specified in [27]. Percentage of the reference allele counts were defined as REF counts/(REF counts + ALT counts) * 100. One sample t test was performed to test whether the ratio is different from the null allelic proportion of 0.5.

2.10. Statistical analysis

Data are expressed as means ± SEMs. Statistical significance was determined by one-way ANOVA followed by Tukey's multiple comparisons test or two-way ANOVA followed by Bonferroni post-test to compare means between groups. Unpaired t test was used for comparison between two groups. Statistical analyses were performed using GraphPad Prism 9 for Mac OS X (GraphPad Software Inc., San Diego, CA).

2.11. Approvals

Donor organs from individuals without type 2 diabetes were obtained with written informed consent and approval of the Human Research Ethics Board of the University of Alberta (Pro00013094; Pro 00001754). All animal studies were approved by the Animal Care and Use Committee at the University of Alberta (AUP00000291, AUP00000405).

3. RESULTS

3.1. Deletion of *Zmiz1* from pancreatic β-cells results in impaired glucose tolerance in mice

To characterize the role of pancreatic β-cell *Zmiz1* on glucose homeostasis, we selectively deleted the *Zmiz1* in β-cells by crossing Ins1-*cre*$^{+}$ [14] with *Zmiz1*$^{fl/fl}$ mice (Figure 1A). β-cell specific knockout (*Ins1-Cre*$^{+}$*Zmiz1*$^{fl/fl}$), heterozygous (*Ins1-Cre*$^{+}$*Zmiz1*$^{fl/+}$) mice, and their control littermates (*Ins1-Cre*$^{+}$*Zmiz1*$^{+/+}$) were generated and referred to as Zmiz1$^{\beta KO}$, Zmiz1$^{\beta HET}$, Zmiz1^{Ctrl}, respectively. All mice, including Zmiz1^{Ctrl}, had Cre recombinase expression in β-cells and was confirmed by breeding the Ins1-*cre*$^{+}$ knock-in mice with ROSA26 Cre reporter mice (*R26R*$^{fl/fl}$) [13] followed by X-gal staining (Suppl Fig. 1A). Loss of Zmiz1 in Zmiz1$^{\beta KO}$ islets was confirmed by RT-qPCR to sequences up- and down-stream of the floxed site (Suppl Fig. 1B), and immunoblotting (Figure 1B). We assessed OGTT, IPGTT and ITT in 12 week old mice on a chow diet (Figure 1C). Both female and male Zmiz1$^{\beta KO}$ mice were glucose intolerant compared with Zmiz1^{Ctrl} littermates (Figure 1D–G). Insulin tolerance of female and male mice was not different across all groups (Suppl Fig. 2), suggesting β-cell specific loss of Zmiz1 does not affect insulin sensitivity. Glucose-stimulated insulin secretion from isolated islets was markedly reduced from both the female and male Zmiz1$^{\beta KO}$ mice (Figure 1H–I),

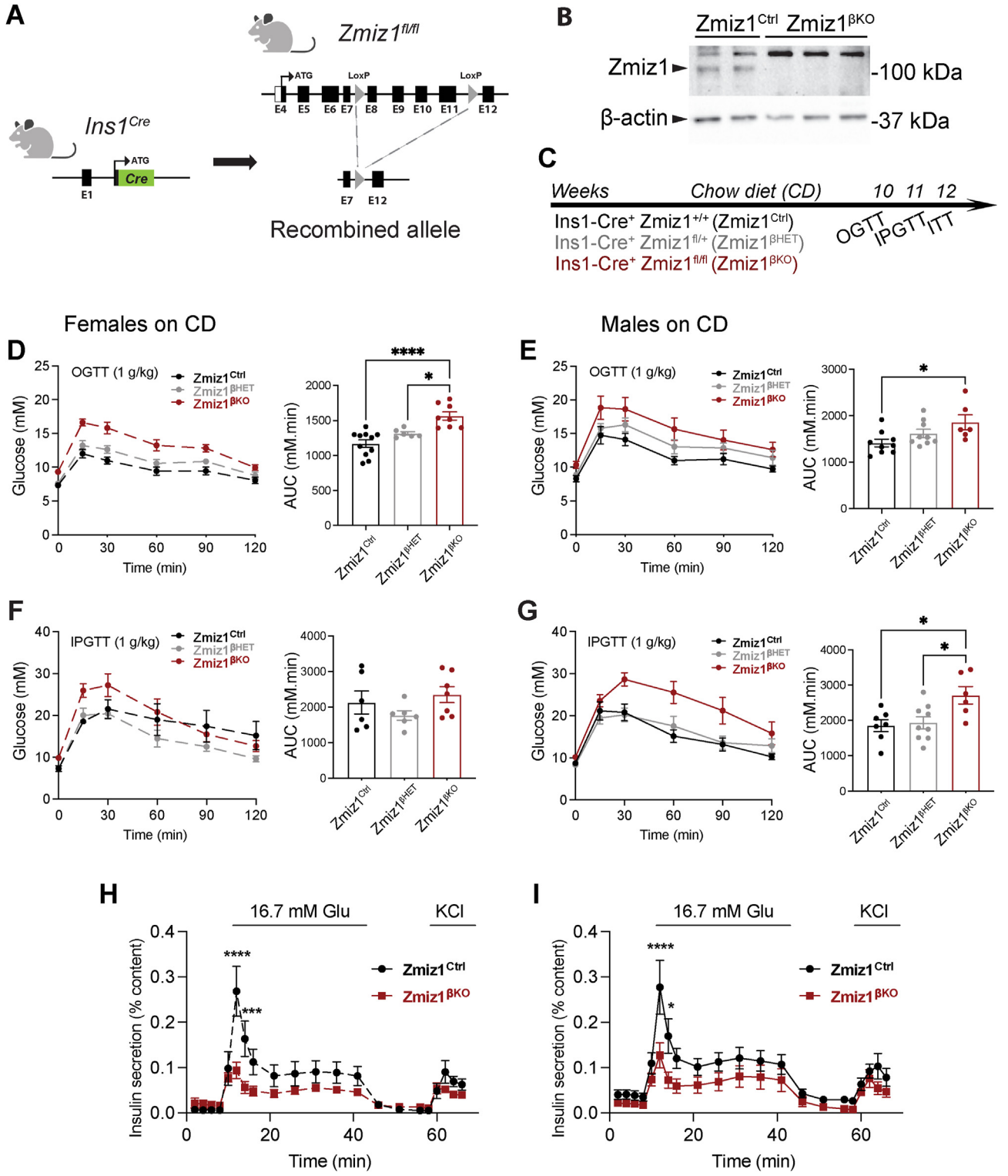

Figure 1: Loss of Zmiz1 in β-cells impairs glucose homeostasis. (A) Schematic of *Ins1*^{Cre} knock-in allele, Zmiz1 floxed allele, and the recombined allele. **(B)** Immunoblotting for Zmiz1 (100 kDa) and β-actin (43 kDa) in lysates of primary islets isolated from *Zmiz1*^{Ctrl} and *Zmiz1*^{βKO} mice. **(C)** Schematic of experimental workflow on chow diet fed mice. **(D–E)** Oral glucose tolerance test (OGTT) and **(F–G)** intraperitoneal glucose tolerance test (IPGTT) in female (n = 6–11 per group) and male (n = 6–9 per group) Zmiz1 knockout and control mice. (**H-I**) Insulin secretion from female **(H)** and male **(I)** *Zmiz1*^{Ctrl} or *Zmiz1*^{βKO} mouse islets in response to glucose (n = 6–10 per group). CD, chow diet. Glu, glucose. AUC, area under the curve. Data are mean ± SEM. $^{*}P < 0.05$, $^{****}P < 0.0001$ by one-way ANOVA followed by Tukey's multiple comparisons test or by two-way ANOVA followed by Bonferroni post-test.

consistent with the lower plasma insulin responses in the Zmiz1$^{\beta KO}$ mice (Suppl Fig. 3).

3.2. *Zmiz1* loss causes dysregulation of genes implicated in β-cell function and maturation

RNA-sequencing was performed on islets from chow fed male and female Zmiz1$^{\beta KO}$ and Zmiz1^{Ctrl} mice at 12 weeks of age (Figure 2A). There were 291 upregulated and 265 downregulated genes in Zmiz1$^{\beta KO}$ islets (padj <0.05) (Figure 2B). Differentially expressed genes by sex are shown in Supplemental Table 1. Key β-cell maturity markers were downregulated (*Mafa*, *Glp1r*, *Slc2a2*, *Nkx6-1*, *Ins2*, *Ins1*) [29], as were genes with known roles in insulin secretion and glucose metabolism (Figure 2C). Several genes implicated in β-cell proliferation and differentiation were also dysregulated (*E2f3*, *Rfx3*, *Nfatc1*, *E2f1*) (Figure 2C) [30–33]. Intriguingly, markers of immature or dedifferentiated β-cells, including *CD81* [34] and *Aldh1a3* [35], were upregulated in the Zmiz1$^{\beta KO}$ islet transcriptome (Figure 2C). Immunoblotting of whole-islet lysates from Zmiz1$^{\beta KO}$ mice, where some continued Zmiz1 expression likely results from expression in non-β-cells, confirmed the upregulation of CD81 and Aldh1a3 (Figure 2D–E), highlighting a potential role for Zmiz1 in maintaining β-cell maturation. To further understand the transcriptional network which Zmiz1 regulates in β-cells, we performed *in silico* analysis to identify the potential transcription factors downstream of Zmiz1. Integrated Motif Activity Response Analysis (ISMARA) uses RNA-seq data to predict key transcription factors driving the observed changes in gene expression (Figure 2F). Among the top-ranked predicted regulatory motifs sorted by activity significance (Z-value) are transcription factors implicated in β-cell proliferation (*Nfatc2*), cell differentiation (*Zfp281* and *Rfx3*), and β-cell function and maturation (*Atf3* and *Atf4*) (Figure 2F–G). It will be important in future studies to examine whether Zmiz1 interacts directly with these potential tragets. Furthermore, although Notch and c-Myc are known targets of Zmiz1 [10,36,37], we did not see altered expression of these genes or their targets in Zmiz1$^{\beta KO}$ islets (Suppl Fig. 4).

3.3. Loss of *Zmiz1* restricts β-cell expansion upon high fat feeding, leading to severe glucose intolerance

We next examined the effect of *Zmiz1* deletion from β cells upon high-fat feeding. 12-week old male and female Zmiz1$^{\beta KO}$ mice and controls were put on high fat diet (HFD) for 8 weeks and OGTT, IPGTT, and ITT were performed (Figure 3A). Both female and male HFD-Zmiz1$^{\beta KO}$ mice developed fasting hyperglycemia and severe glucose intolerance by 20 weeks of age (Figure 3B–C). In males, glucose intolerance measured by IPGTT (Figure 3D) was more obvious than female HFD-Zmiz1$^{\beta KO}$ mice (Suppl Fig. 5A) where we observed much less induction of insulin intolerance (Suppl Fig. 5B) than in male mice (Figure 3E). Fasting insulin is increased upon HFD in males (Figure 3F), but this increase is much less in females (Suppl Fig. 5C), likely due to their resistance to developing insulin intolerance. The development of fasting hyperinsulinema was blunted in the male HFD-Zmiz1^{HET} and HFD-Zmiz1$^{\beta KO}$ mice (Figure 3F). In the female HFD-Zmiz1^{HET} and HFD-Zmiz1$^{\beta KO}$ mice, we observed a small increase in fasting plasma insulin levels compared with HFD-Zmiz1^{Ctrl} (Suppl Fig. 5C), although the nature of this remains unclear. To investigate the underlying mechanism, we assessed β-cell mass in HFD-Zmiz1$^{\beta KO}$ mice, and littermate controls. Consistent with the resistance of female mice to HFD-induced glucose intolerance [38] and insulin resistance, and thus a lower driving force for β-cell mass expansion, we see little difference in β-cell mass in the female HFD-Zmiz1$^{\beta KO}$ mice (Suppl Fig. 5D–E). In males, however, while β-cell mass is not different upon chow feeding, the expansion seen with HFD in controls is markedly reduced in male HFD-Zmiz1$^{\beta KO}$ mice (Figure 3G–H). Glucose-stimulated insulin secretion was not different in both male and female HFD-Zmiz1$^{\beta KO}$ mice compared to control (Suppl Fig. 5F–G). Given that the *in vitro* secretion assay normalizes responses to similar numbers of hand-picked islets (of relatively similar size), these observations suggest that hyperglycemia in the HFD-Zmiz1$^{\beta KO}$ mice is primarily driven by an impaired islet mass expansion.

3.4. T2D risk alleles at the *ZMIZ1* locus are associated with reduced insulin content and secretion in primary human islets

We assessed secretory phenotypes in isolated islets from carriers of T2D risk variants at *ZMIZ1* in a cohort of 232 donors without diabetes (Figure 4). There are two independent T2D-association signals at the *ZMIZ1* locus, one of which has been fine mapped to a ~11 kb interval and contains 10 SNPs in the credible set including the lead SNP rs703972 (Figure 4A) and the previously reported eQTL rs12571751 [39,40]. The sex distribution, age, body mass index, and HbA1c were not different among genotypes (Suppl Figs. 6 and 7). Islets from homozygous carriers of the T2D-risk alleles at rs703972 (G allele) and rs12571751 (A allele) had significantly lower insulin content compared to noncarriers (Figure 4B–C). Although no differences were observed in insulin secretion at low glucose (1 mM) concentrations, there was a reduction in insulin secretion in response to high glucose (16.7 mM), in the T2D risk-allele carriers (Figure 4D–E). The second signal has been fine mapped to an ~834 kb interval containing 861 variants in the credible set. There was no similar effect of the lead SNP (rs1317617) at this second locus, which may point to another effector gene at this signal (Suppl Fig. 6E–F). Separation of these data by sex gave directionally consistent results for both sexes, but a loss of statistical power (Suppl Fig. 7).

To understand how T2D risk alleles at the first signal could alter *ZMIZ1* expression and to determine which SNP is functional at the locus, we explored allelic differences in chromatin accessibility for credible set variants. We accessed publically available ATAC-seq data from 17 human islet donors and identified heterozygous individuals for three (rs703977, rs12571751, and rs810517) credible set variants which met our criteria (read depth ≥ 5 for each allele and >2 heterozygous donors) for inclusion in the analysis. No heterozygous carriers of the lead SNP rs703972 had sufficient read depth for inclusion in the analysis. After correcting for potential mapping biases using WASP [41], there was a significant imbalance in allelic-specific chromatin accessibility for rs703977 ($p = 0.02$) with the T2D-risk allele (T) having more open chromatin (Table 1), which would suggest that the T2D-risk allele results in increased *ZMIZ1* expression and is consistent with our previously published eQTL analysis [5]. Finally, we assessed the transcriptional activity of both variants using luciferase assays in the human β-cell line, EndoC-βH1 [58]. For both variants, the non-risk allele significantly repressed luciferase activity when cloned in the reverse direction (Suppl Fig. 8), suggesting that the region represses transcription. For the rs703972, the repressive activity is lost with the T2D-risk G allele, although this did not reach statistical significance (Suppl Fig. 8).

4. DISCUSSION

Recent efforts to identify causal variants associated with T2D risk require parallel efforts to identify the mechanisms underpinning these association signals that will be crucial for accelerating translation of T2D genetic discoveries into clinical applications. In the current study, we characterized the functional role of the T2D risk gene *ZMIZ1* in pancreatic β-cells.

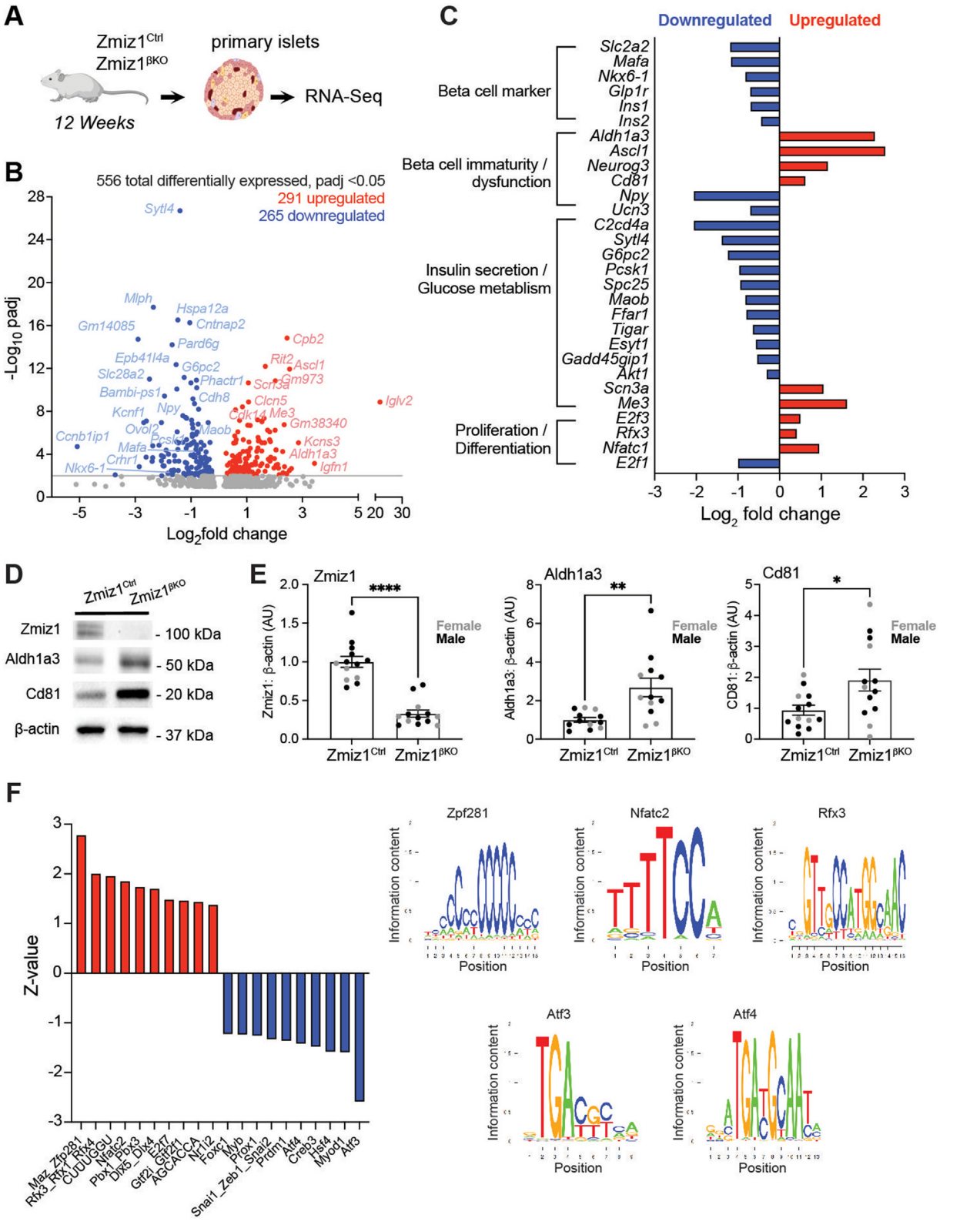

Figure 2: *Zmiz1* loss in β-cells results in dysregulation of genes implicated in β-cell function and maturation. (A) Schematic of experimental workflow of RNA-seq of mouse islets from chow fed female *Zmiz1*^{Ctrl} (n = 3), female *Zmiz1*^{βKO} (n = 4), male *Zmiz1*^{Ctrl} (n = 4), and male *Zmiz1*^{βKO} (n = 3) mice. **(B)** Volcano plot of the differentially expressed genes in *Zmiz1*^{βKO} islets. **(C)** Selected differentially expressed genes from the RNA-seq data and their known cellular functions. **(D)** Immunoblotting for Zmiz1, Aldh1a3, Cd81, and β-actin in lysates of primary islets from *Zmiz1*^{Ctrl} or *Zmiz1*^{βKO} mice. **(E)** Quantification of band intensity of the indicated proteins in lysates of primary islets from *Zmiz1*^{Ctrl} (n = 13) or *Zmiz1*^{βKO} (n = 13) mice. **(F)** ISMARA analysis of top transcription factor binding motifs based on their motif activity (Z-value). **(G)** Selected predicted transcription factor binding motifs displayed. Data are mean ± SEM. $*P < 0.05$, $***P < 0.001$ by student t test. Upregulated (red). Downregulated (blue). (For interpretation of the references to color in this figure legend, the reader is referred to the Web version of this article.)

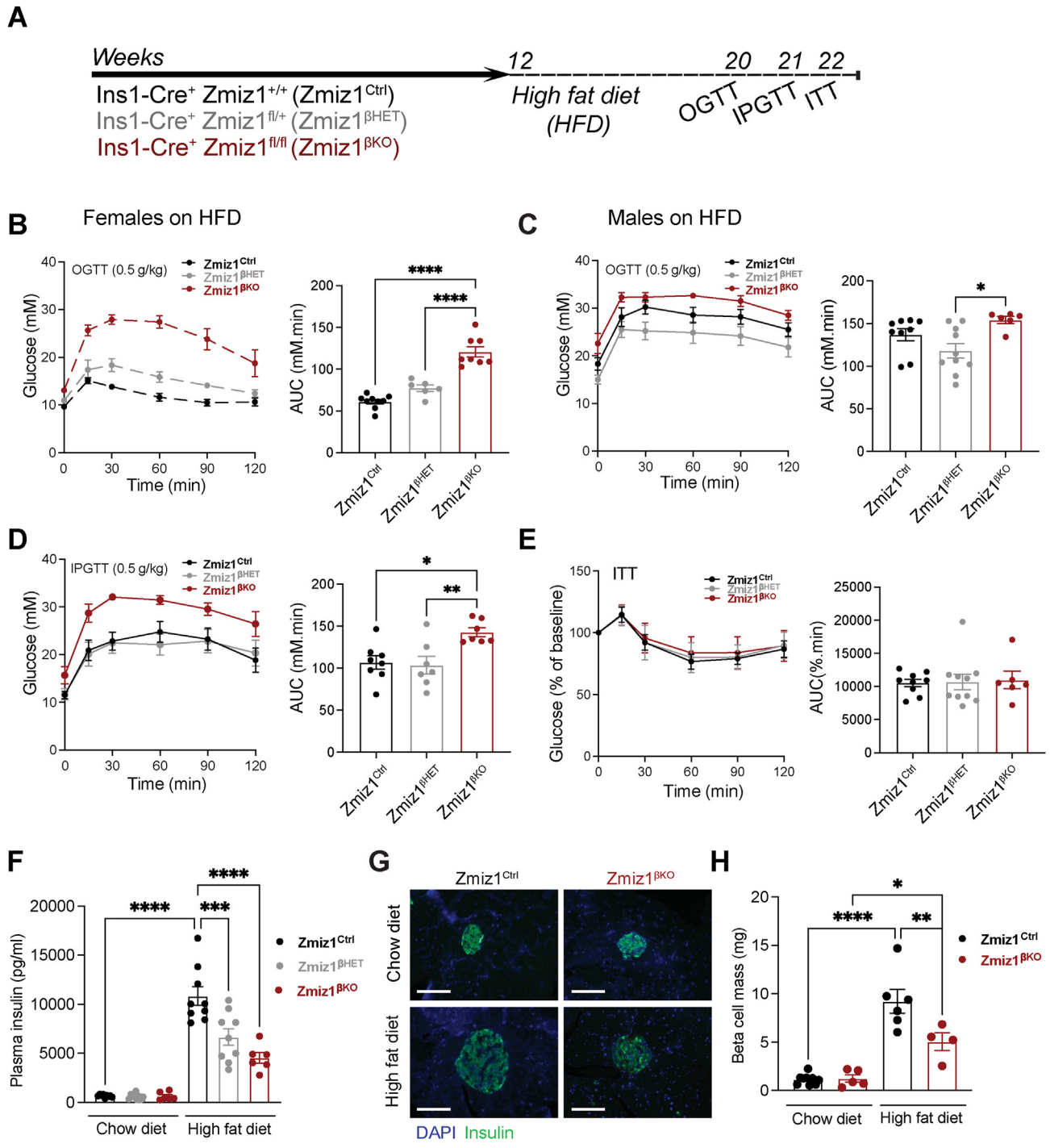

Figure 3: Loss of *Zmiz1* in β-cells reduces β-cell mass and worsens impaired glucose tolerance in mice challenged with high fat diet. (A) Schematic of experimental workflow on high fat diet (HFD) fed mice. **(B)** Oral glucose tolerance test (OGTT) in female *Zmiz1* knockout and control mice (n = 6–9 per group). **(C-F)** Oral glucose tolerance test (OGTT) (**C**), intraperitoneal glucose tolerance test (IPGTT) (D), insulin tolerance test (ITT) (**E**), fasting plasma insulin following OGTT (**F**), in male control and $Zmiz1^{\beta KO}$ mice (n = 6–10 per group). **(G)** Representative immunostaining image of β-cell mass in $Zmiz1^{Ctrl}$ and $Zmiz1^{\beta KO}$ mice fed with HFD (scale bars = 100 μm). **(H)** β-cell mass relative to pancreas weight in $Zmiz1^{Ctrl}$ (n = 6) and $Zmiz1^{\beta KO}$ (n = 4) mice following HFD. Average of 3–4 pancreatic sections per animal was considered one replicate. Insulin (green), nuclei (blue). HFD, high fat diet. AUC, area under the curve. Data are mean ± SEM. $^{*}P < 0.05$, $^{**}P < 0.01$, $^{***}P < 0.001$, $^{****}P < 0.0001$ by one-way ANOVA followed by Tukey's multiple comparisons test. (For interpretation of the references to color in this figure legend, the reader is referred to the Web version of this article.)

In chow-fed mice, β-cell specific deletion of *Zmiz1* results in glucose intolerance with no change in insulin sensitivity, highlighting an important role of Zmiz1 in maintaining glucose homeostasis. In these animals, impaired glucose tolerance following loss of β-cell *Zmiz1* likely results from reduced glucose-stimulated insulin secretion as β-cell mass was unaffected in the $Zmiz1^{\beta KO}$ mice. Following high fat feeding, glucose-stimulated insulin responses seem equally poor, and impaired fasting glucose is driven by an impaired β-cell mass

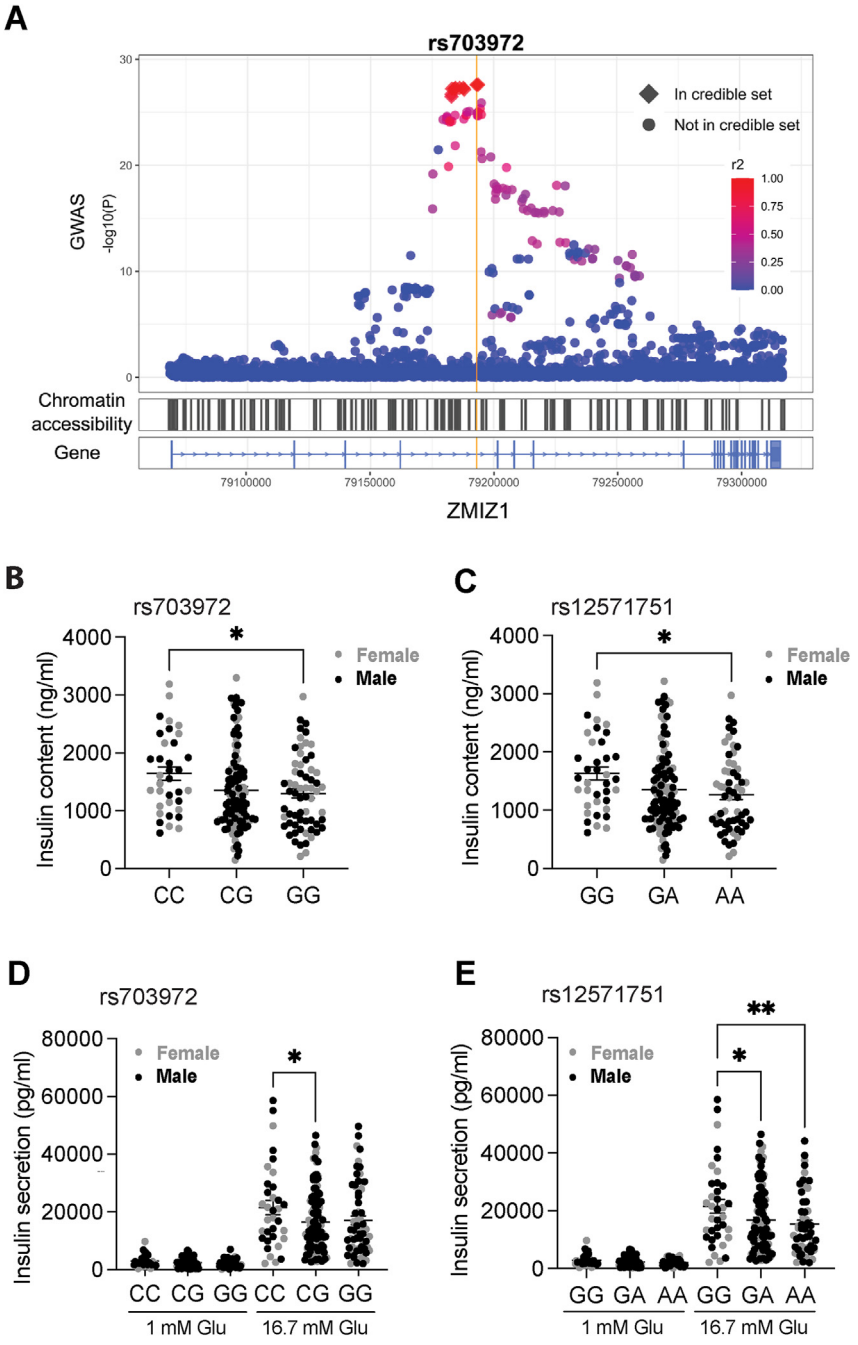

Figure 4: Effect of the T2D-associated alleles at the *ZMIZ1* locus on insulin secretion in primary human islets from donors without diabetes. (A) Locus zoom plot for the *ZMIZ1* locus. The 10 SNPs in the 99% credible set defined by Mahajan et al. [28] are shown as diamonds. LD r2 values are from the European population in TopLD. The lead SNP (rs703972) at the signal is shown with the yellow line. Chromatin accessibility in human islets is shown with open chromatin indicated by black lines. **(B-C)** Total insulin content in human islets from genotyped human donors. **(D—E)** Insulin secretion in response to low glucose (1 mM) or high glucose (16.7 mM) by *ZMIZ1* genotype at the lead SNP (rs703972) and previously reported eQTL (rs12571751). rs703972 CC, n = 37; CG, n = 126; GG, n = 69 where G is the risk allele. rs12571751 GG, n = 39; GA, n = 127; AA, n = 66 where A is the risk allele. Sex, age, BMI and HbA1c distribution is shown in Suppl Fig. 6. Data separated by sex are shown in Suppl Fig. 7. Glu, glucose. Data are mean ± SEM. $*P < 0.05$, $**P < 0.01$ by one-way ANOVA followed by Tukey's multiple comparisons test. (For interpretation of the references to color in this figure legend, the reader is referred to the Web version of this article.)

expansion and lower fasting insulin in the male (but not female) *Zmiz1*$^{\beta KO}$ mice. This sex-difference is likely secondary to the resistance of females to developing an insulin resistance on the high fat diet. Our RNA-seq analysis showed that *Zmiz1* absence in β-cells results in downregulation of mature β-cell markers and upregulation of immature and dedifferentiated β-cell markers including *Aldh1a3* and *Cd81*. The enzyme aldehyde dehydrogenase 1 isoform A3 (ALDH1A3) has been shown to mark dysfunctional β-cells that have progenitor like features including the expression of *Neurgo3* [35], which itself was upregulated in Zmiz1$^{\beta KO}$ islets. CD81 has been recently identified as a

Table 1 — Allelic imbalance in open chromatin of T2D-associated variants in *ZMIZ1*.

Variant	DIAGRAM P-value	Fgwas T2D PPA	Allelic imbalance Allele Ratio (Allele #)	Allelic imbalance WASP P-value	T2D risk allele	Chromatin state of risk allele
rs12571751	3.3E−27	1.5E−02	0.43 (52A VS 68G alleles)	0.59	A	No difference
rs703977	5.0E−28	1.1E−01	0.65 (95T VS 52G alleles)	0.02	T	↑ Open
rs810517	2.0E−27	2.6E−02	0.49 (49C VS 52T alleles)	0.65	C	No difference

novel surface marker for immature and de-differentiated β-cells in the adult mouse and human islets [34]. Salinno et al. showed that subpopulation of high CD81 expressing mouse β-cells have low expression levels of the mature β-cell marker *Ucn3*, which we also find to be downregulated in the Zmiz1$^{\beta KO}$ islets. Moreover, a similar expression pattern of *Cd81* and *Aldh1a3* was reported in STZ-diabetic mouse β-cells [34]. In our study, we confirmed the upregulation of both CD81 and ALDH1A3 at the protein level in adult Zmiz1$^{\beta KO}$ islets, which demonstrates a role for Zmiz1 in β-cell maturation.

The implication of Zmiz1 in β-cell maturation is further supported by the upregulation of the transcription factor *Rfx3* in Zmiz1$^{\beta KO}$ islet transcriptome profile and in the ISMARA analysis. This is likely a compensatory effect since RFX3 plays an essential role in the differentiation and function of mature β-cells [30]. Although it is not clear how Zmiz1 contributes to the establishment or maintenance of β-cell maturity, our ISMARA analysis implicates the transcription factors ATF3 and ATF4, master regulators of the cellular stress response with dual roles in glucose homeostasis [42–44]. The role of ATF3 is tissue-specific and context-dependant [43]. Several studies reported a protective role of ATF3 in β-cells [45,46]. ATF3 deficiency in HFD-fed mice exacerbates glucose intolerance and impairs insulin secretion without affecting β-cell mass [44]. ATF3 is known to be regulated by ATF4 [44], which has recently been shown to play a protective role in diabetic Akita mice by preserving β-cell identity [47]. However, while β-cell specific deletion of *Atf4* in Akita mice resulted in β-cell dedifferentiation, this was hardly seen in β-cell specific knockout of *Atf4* in non-diabetic mice although β-cell proliferation was markedly reduced [47].

A role of Zmiz1 in T cell-development by regulating Notch signalling has been previously reported [10]. Although Notch signalling plays a role in β-cell maturation [48,49], altered expression of Notch target genes were not observed in the *Zmiz1*$^{\beta KO}$ islet transcriptome and we see no change in Notch protein expression in islets from chow-fed *Zmiz1*$^{\beta KO}$ mice. In zebrafish, inactivating CRISPR/Cas9 mutations in the *zmiz1a* gene results in lethality at 15 days post fertilization and delayed erythroid maturation, demonstrating a crucial role of *Zmiz1a* in terminal differentiation of erythrocytes [50]. The authors also showed that loss of *Zmiz1a* in zebrafish caused a dysregulation in autophagy [50]. Dysregulation of autophagy genes was not observed in *Zmiz1*$^{\beta KO}$ islet transcriptome with the exception of the autophagy gene *Atg4d,* which was downregulated. Thus, although Zmiz1 has been implicated in cellular development through Notch and autophagy pathways, we find no evidence supporting these pathways within the islet.

Among the potential Zmiz1 binding transcription factors predicted by ISMARA analysis is the suppressor Znf281, a zinc-finger transcription factor that regulates embryonic stem cells differentiation by acting as a repressor of many stem cell pluripotency genes [51]. Znf281 has been shown to inhibit differentiation of cortical neurons [52]. Accordingly, a possible mechanism by which Zmiz1 maintains β-cell maturity is through activation of transcriptional suppressors of genes associated with de-differentiated cell state such as Znf281.

Severe glucose intolerance was observed, particularly in response to oral glucose, in both male and female *Zmiz1*$^{\beta KO}$ mice subjected to HFD-feeding for 8 weeks. The worsened glucose intolerance in response to oral compared to IP glucose suggests an implication of incretin response, which is known to be enhanced following HFD [53–55]. This is consistent with our previous observations in HFD-mouse models [20]. In male *Zmiz1*$^{\beta KO}$ mice, HFD feeding resulted in impaired β-cell mass expansion and reduced fasting insulin levels compared to controls. Notably, Nfatc1/2, among the differentially expressed genes and the top-ranked Zmiz1-binding candidate, is known to promote β-cell proliferation in mouse and human islets [33,56]. The β-cell mass phenotype was less obvious in females, and accordingly, the fasting hyperglycaemia was much more pronounced in males. This is not necessarily due to sex-differences in Zmiz1 impacts on islet mass. While Zmiz1 interacts with the androgen receptor (AR), male mice with specific deletion of the *Ar* in β-cells showed no obvious defect in islet mass or mass expansion upon metabolic stress [57]. The HFD-fed female mice were more resistant to the development of insulin resistance and glucose intolerance, consistent with previous reports that female mice are protected against HFD-induced metabolic changes [20,38], and therefore, islet mass expanded very little in the female controls.

In humans, we demonstrate that islets from carriers of T2D-risk alleles at the *ZMIZ1* locus have reduced insulin content and insulin secretion in response to high glucose compared with noncarriers, suggesting a key role for ZMIZ1 in β-cell function in humans. Although not conclusive, our efforts to provide a direction of effect at the *ZMIZ1* locus through islet genomics continue to support a role for increased expression as a cause for elevated diabetes risk. The allelic imbalance of chromatin accessibility at rs703977 supports the T2D-risk allele impacting islet function through increased *ZMIZ1* expression. The identification of chromatin QTLs at this locus in larger numbers of islet samples would strengthen this observation. Consistent with these findings, we now show that the region harbouring these diabetes associated variants acts as a transcriptional repressor. Our findings are in line with our previous studies demonstrating that perturbation of *ZMIZ1* expression in human islets and β-cells negatively influences insulin secretion [5,12]. In human islets, both *ZMIZ1* overexpression and knockdown reduced insulin secretion [5], although the effect of partial knockdown (40% of control) was modest, resulting in a ∼10% reduction in insulin secretion in response to KCl-stimulation. In a follow up study, knockdown of *ZMIZ1* in the human β-cell line EndoC-βH1 lead to a reproducible reduction in insulin secretion and cell count [12]. Taken together, these data suggest that *ZMIZ1* levels are precisely regulated to support robust insulin secretion. The relatively modest *ZMIZ1* knockdown in human islets [5] could account for the differences observed between those experiments and the *Zmiz1*$^{\beta KO}$ mice. Alternatively, the acute knockdown of *ZMIZ1* may have been of insufficient duration and at an inappropriate time point to observe a clear secretory defect, given current data supporting a role for Zmiz1 in β-cell maturation.

In summary, our findings demonstrate that ZMIZ1 is crucial for β-cell function and glucose homeostasis and suggest a speculative model by which ZMIZ1 controls a dynamic transcriptional network that governs β-cell maturity and function. Future studies aimed at understanding

how ZMIZ1 maintains β-cell functional maturity will be crucial for filling major knowledge gap in current β-cell differentiation protocols for cell replacement therapy.

FUNDING

This study was funded by a grant from the Canadian Institutes of Health Research (CIHR: 148451) to PEM. Work in Oxford and Stanford was funded by the Wellcome (200837) and National Institute of Diabetes and Digestive and Kidney Diseases (U01-DK105535; U01-DK085545, UM1DK126185, U01DK123743, U24DK098085) and the Stanford Diabetes Research Center (NIDDK award P30DK116074). ALG is a Wellcome Senior Research Fellow. PEM holds the Canada Research Chair in Islet Biology.

AUTHOR CONTRIBUTIONS

TAA: Performed experiments and analyzed data. Wrote the manuscript.
NAJK: Performed experiments and analyzed data. Wrote and edited the manuscript.
NS, AFS, VR, AJ, HS, MF, KS, JY, JEMF: Performed experiments and analyzed data.
ZS: Designed and generated the floxed Zmiz1 mouse line
ALG: Conceived the study and oversaw the research; Edited the manuscript
PEM: Conceived the study, oversaw the research, edited the manuscript, and acts as guarantor.

DATA AVAILABILITY

Data will be made available on request.

ACKNOWLEDGEMENTS

The University of Alberta is situated on Treaty 6 territory, traditional lands of First Nations and Métis people. We thank Sameena Nawaz (Oxford) for assistance with RNA preparation. We thank the Human Organ Procurement and Exchange (HOPE) program and Trillium Gift of Life Network (TGLN) for their work in procuring human donor pancreas for research, and James Lyon (Edmonton) and Austin Bautista (Edmonton) for their work in human islet isolation at the Alberta Diabetes Institute IsletCore (www.isletcore.ca). We especially thank the organ donors and their families for their kind gift in support of diabetes research.

CONFLICT OF INTEREST

The authors have no relevant conflicts of interest to disclose.

APPENDIX A. SUPPLEMENTARY DATA

Supplementary data to this article can be found online at https://doi.org/10.1016/j.molmet.2022.101621.

REFERENCES

[1] Krentz, N.A.J., Gloyn, A.L., 2020. Insights into pancreatic islet cell dysfunction from type 2 diabetes mellitus genetics. Nature Reviews. Endocrinology 16(4): 202–212. https://doi.org/10.1038/s41574-020-0325-0.

[2] Mahajan, A., Spracklen, C.N., Zhang, W., Ng, M.C.Y., Petty, L.E., Kitajima, H., et al., 2022. Multi-ancestry genetic study of type 2 diabetes highlights the power of diverse populations for discovery and translation. Nature Genetics 54(5):560–572. https://doi.org/10.1038/s41588-022-01058-3.

[3] Spracklen, C.N., Horikoshi, M., Kim, Y.J., Lin, K., Bragg, F., Moon, S., et al., 2020. Identification of type 2 diabetes loci in 433,540 East Asian individuals. Nature 582(7811):240–245. https://doi.org/10.1038/s41586-020-2263-3.

[4] Viñuela, A., Varshney, A., van de Bunt, M., Prasad, R.B., Asplund, O., Bennett, A., et al., 2020. Genetic variant effects on gene expression in human pancreatic islets and their implications for T2D. Nature Communications 11(1): 4912. https://doi.org/10.1038/s41467-020-18581-8.

[5] van de Bunt, M., Manning Fox, J.E., Dai, X., Barrett, A., Grey, C., Li, L., et al., 2015. Transcript expression data from human islets links regulatory signals from genome-wide association studies for type 2 diabetes and glycemic traits to their downstream effectors. PLoS Genetics 11(12):e1005694. https://doi.org/10.1371/journal.pgen.1005694.

[6] Sharma, M., Li, X., Wang, Y., Zarnegar, M., Huang, C.-Y., Palvimo, J.J., et al., 2003. hZimp10 is an androgen receptor co-activator and forms a complex with SUMO-1 at replication foci. The EMBO Journal 22(22):6101–6114. https://doi.org/10.1093/emboj/cdg585.

[7] Shuai, K., Liu, B., 2005. Regulation of gene-activation pathways by PIAS proteins in the immune system. Nature Reviews. Immunology 5(8):593–605. https://doi.org/10.1038/nri1667.

[8] Lee, J., Beliakoff, J., Sun, Z., 2007. The novel PIAS-like protein hZimp10 is a transcriptional co-activator of the p53 tumor suppressor. Nucleic Acids Research 35(13):4523–4534. https://doi.org/10.1093/nar/gkm476.

[9] Li, X., Thyssen, G., Beliakoff, J., Sun, Z., 2006. The novel PIAS-like protein hZimp10 enhances Smad transcriptional activity. The Journal of Biological Chemistry 281(33):23748–23756. https://doi.org/10.1074/jbc.M508365200.

[10] Pinnell, N., Yan, R., Cho, H.J., Keeley, T., Murai, M.J., Liu, Y., et al., 2015. The PIAS-like coactivator Zmiz1 is a direct and selective cofactor of Notch1 in T cell development and leukemia. Immunity 43(5):870–883. https://doi.org/10.1016/j.immuni.2015.10.007.

[11] Beliakoff, J., Lee, J., Ueno, H., Aiyer, A., Weissman, I.L., Barsh, G.S., et al., 2008. The PIAS-like protein Zimp10 is essential for embryonic viability and proper vascular development. Molecular and Cellular Biology 28(1):282–292. https://doi.org/10.1128/MCB.00771-07.

[12] Thomsen, S.K., Ceroni, A., van de Bunt, M., Burrows, C., Barrett, A., Scharfmann, R., et al., 2016. Systematic functional characterization of candidate causal genes for type 2 diabetes risk variants. Diabetes 65(12): 3805–3811. https://doi.org/10.2337/db16-0361.

[13] Soriano, P., 1999. Generalized lacZ expression with the ROSA26 Cre reporter strain. Nature Genetics 21(1):70–71. https://doi.org/10.1038/5007.

[14] Thorens, B., Tarussio, D., Maestro, M.A., Rovira, M., Heikkilä, E., Ferrer, J., 2015. Ins1(Cre) knock-in mice for beta cell-specific gene recombination. Diabetologia 58(3):558–565. https://doi.org/10.1007/s00125-014-3468-5.

[15] Smith, N., Ferdaoussi, M., Lin, H., E Macdonald, P., 2018. Oral glucose tolerance test in mouse v1.

[16] Smith, N., Ferdaoussi, M., Lin, H., E Macdonald, P., 2019. IP glucose tolerance test in mouse v1.

[17] Smith, N., Ferdaoussi, M., Lin, H., E Macdonald, P., 2019. Insulin tolerance test in mouse v1.

[18] Smith, N., F Spigelman, A., Lin, H., E Macdonald, P., 2018. Mouse pancreatic islet isolation v1.

[19] Smith, N., Lin, H., Ferdaoussi, M., E Macdonald, P., 2018. Purification of mouse pancreatic islets using histopaque gradient centrifugation v1.

[20] Lin, H., Smith, N., Spigelman, A.F., Suzuki, K., Ferdaoussi, M., Alghamdi, T.A., et al., 2021. β-Cell knockout of SENP1 reduces responses to incretins and worsens oral glucose tolerance in high-fat diet-fed mice. Diabetes 70(11): 2626–2638. https://doi.org/10.2337/db20-1235.

[21] Dobin, A., Gingeras, T.R., 2015. Mapping RNA-seq reads with STAR. Current Protocols in Bioinformatics 51(1). https://doi.org/10.1002/0471250953.bi1114s51.

[22] Liao, Y., Smyth, G.K., Shi, W., 2014. featureCounts: an efficient general purpose program for assigning sequence reads to genomic features. Bioinformatics 30(7):923–930. https://doi.org/10.1093/bioinformatics/btt656.

[23] Ritchie, M.E., Phipson, B., Wu, D., Hu, Y., Law, C.W., Shi, W., et al., 2015. Limma powers differential expression analyses for RNA-sequencing and microarray studies. Nucleic Acids Research 43(7). https://doi.org/10.1093/nar/gkv007 e47–e47.

[24] Love, M.I., Huber, W., Anders, S., 2014. Moderated estimation of fold change and dispersion for RNA-seq data with DESeq2. Genome Biology 15(12):550. https://doi.org/10.1186/s13059-014-0550-8.

[25] Balwierz, P.J., Pachkov, M., Arnold, P., Gruber, A.J., Zavolan, M., van Nimwegen, E., 2014. ISMARA: automated modeling of genomic signals as a democracy of regulatory motifs. Genome Research 24(5):869–884. https://doi.org/10.1101/gr.169508.113.

[26] Lyon, J., F Spigelman, A., E Macdonald, P., E Manning Fox, J., 2019. ADI IsletCore protocols for the isolation, assessment and cryopreservation of human pancreatic islets of langerhans for research purposes v1.

[27] Thurner, M., van de Bunt, M., Torres, J.M., Mahajan, A., Nylander, V., Bennett, A.J., et al., 2018. Integration of human pancreatic islet genomic data refines regulatory mechanisms at Type 2 Diabetes susceptibility loci. ELife 7: e31977. https://doi.org/10.7554/eLife.31977.

[28] Mahajan, A., Taliun, D., Thurner, M., Robertson, N.R., Torres, J.M., Rayner, N.W., et al., 2018. Fine-mapping type 2 diabetes loci to single-variant resolution using high-density imputation and islet-specific epigenome maps. Nature Genetics 50(11):1505–1513. https://doi.org/10.1038/s41588-018-0241-6.

[29] Salinno, C., Cota, P., Bastidas-Ponce, A., Tarquis-Medina, M., Lickert, H., Bakhti, M., 2019. β-Cell maturation and identity in Health and disease. International Journal of Molecular Sciences 20(21):E5417. https://doi.org/10.3390/ijms20215417.

[30] Ait-Lounis, A., Bonal, C., Seguín-Estévez, Q., Schmid, C.D., Bucher, P., Herrera, P.L., et al., 2010. The transcription factor Rfx3 regulates beta-cell differentiation, function, and glucokinase expression. Diabetes 59(7):1674–1685. https://doi.org/10.2337/db09-0986.

[31] Fajas, L., Annicotte, J.-S., Miard, S., Sarruf, D., Watanabe, M., Auwerx, J., 2004. Impaired pancreatic growth, beta cell mass, and beta cell function in E2F1 (–/–)mice. The Journal of Clinical Investigation 113(9):1288–1295. https://doi.org/10.1172/JCI18555.

[32] Rady, B., Chen, Y., Vaca, P., Wang, Q., Wang, Y., Salmon, P., et al., 2013. Overexpression of E2F3 promotes proliferation of functional human β cells without induction of apoptosis. Cell Cycle 12(16):2691–2702. https://doi.org/10.4161/cc.25834.

[33] Simonett, S.P., Shin, S., Herring, J.A., Bacher, R., Smith, L.A., Dong, C., et al., 2021. Identification of direct transcriptional targets of NFATC2 that promote β cell proliferation. The Journal of Clinical Investigation 131(21):e144833. https://doi.org/10.1172/JCI144833.

[34] Salinno, C., Büttner, M., Cota, P., Tritschler, S., Tarquis-Medina, M., Bastidas-Ponce, A., et al., 2021. CD81 marks immature and dedifferentiated pancreatic β-cells. Molecular Metabolism 49:101188. https://doi.org/10.1016/j.molmet.2021.101188.

[35] Kim-Muller, J.Y., Fan, J., Kim, Y.J.R., Lee, S.-A., Ishida, E., Blaner, W.S., et al., 2016. Aldehyde dehydrogenase 1a3 defines a subset of failing pancreatic β cells in diabetic mice. Nature Communications 7:12631. https://doi.org/10.1038/ncomms12631.

[36] Rakowski, L.A., Garagiola, D.D., Li, C.M., Decker, M., Caruso, S., Jones, M., et al., 2013. Convergence of the ZMIZ1 and NOTCH1 pathways at C-MYC in acute T lymphoblastic leukemias. Cancer Research 73(2):930–941. https://doi.org/10.1158/0008-5472.CAN-12-1389.

[37] Wang, Q., Yan, R., Pinnell, N., McCarter, A.C., Oh, Y., Liu, Y., et al., 2018. Stage-specific roles for Zmiz1 in Notch-dependent steps of early T-cell development. Blood 132(12):1279–1292. https://doi.org/10.1182/blood-2018-02-835850.

[38] Pettersson, U.S., Waldén, T.B., Carlsson, P.-O., Jansson, L., Phillipson, M., 2012. Female mice are protected against high-fat diet induced metabolic syndrome and increase the regulatory T cell population in adipose tissue. PloS One 7(9):e46057. https://doi.org/10.1371/journal.pone.0046057.

[39] Andersen, M.K., Sterner, M., Forsén, T., Käräjämäki, A., Rolandsson, O., Forsblom, C., et al., 2014. Type 2 diabetes susceptibility gene variants predispose to adult-onset autoimmune diabetes. Diabetologia 57(9):1859–1868. https://doi.org/10.1007/s00125-014-3287-8.

[40] Matsuba, R., Sakai, K., Imamura, M., Tanaka, Y., Iwata, M., Hirose, H., et al., 2015. Replication study in a Japanese population to evaluate the association between 10 SNP loci, identified in European genome-wide association studies, and type 2 diabetes. PLOS ONE 10(5):e0126363. https://doi.org/10.1371/journal.pone.0126363.

[41] van de Geijn, B., McVicker, G., Gilad, Y., Pritchard, J.K., 2015. WASP: allele-specific software for robust molecular quantitative trait locus discovery. Nature Methods 12(11):1061–1063. https://doi.org/10.1038/nmeth.3582.

[42] Juliana, C.A., Yang, J., Cannon, C.E., Good, A.L., Haemmerle, M.W., Stoffers, D.A., 2018. A PDX1-ATF transcriptional complex governs β cell survival during stress. Molecular Metabolism 17:39–48. https://doi.org/10.1016/j.molmet.2018.07.007.

[43] Ku, H.-C., Cheng, C.-F., 2020. Master regulator activating transcription factor 3 (ATF3) in metabolic homeostasis and cancer. Frontiers in Endocrinology 11: 556. https://doi.org/10.3389/fendo.2020.00556.

[44] Wortel, I.M.N., van der Meer, L.T., Kilberg, M.S., van Leeuwen, F.N., 2017. Surviving stress: modulation of ATF4-mediated stress responses in normal and malignant cells. Trends in Endocrinology and Metabolism: TEM 28(11):794–806. https://doi.org/10.1016/j.tem.2017.07.003.

[45] Gurzov, E.N., Barthson, J., Marhfour, I., Ortis, F., Naamane, N., Igoillo-Esteve, M., et al., 2012. Pancreatic β-cells activate a JunB/ATF3-dependent survival pathway during inflammation. Oncogene 31(13):1723–1732. https://doi.org/10.1038/onc.2011.353.

[46] Zmuda, E.J., Qi, L., Zhu, M.X., Mirmira, R.G., Montminy, M.R., Hai, T., 2010. The roles of ATF3, an adaptive-response gene, in high-fat-diet-induced diabetes and pancreatic beta-cell dysfunction. Molecular Endocrinology 24(7): 1423–1433. https://doi.org/10.1210/me.2009-0463.

[47] Kitakaze, K., Oyadomari, M., Zhang, J., Hamada, Y., Takenouchi, Y., Tsuboi, K., et al., 2021. ATF4-mediated transcriptional regulation protects against β-cell loss during endoplasmic reticulum stress in a mouse model. Molecular Metabolism 54:101338. https://doi.org/10.1016/j.molmet.2021.101338.

[48] Bartolome, A., Zhu, C., Sussel, L., Pajvani, U.B., 2019. Notch signaling dynamically regulates adult β cell proliferation and maturity. The Journal of Clinical Investigation 129(1):268–280. https://doi.org/10.1172/JCI98098.

[49] Dror, V., Nguyen, V., Walia, P., Kalynyak, T.B., Hill, J.A., Johnson, J.D., 2007. Notch signalling suppresses apoptosis in adult human and mouse pancreatic islet cells. Diabetologia 50(12):2504–2515. https://doi.org/10.1007/s00125-007-0835-5.

[50] Castillo-Castellanos, F., Ramírez, L., Lomelí, H., 2021. zmiz1a zebrafish mutants have defective erythropoiesis, altered expression of autophagy genes, and a deficient response to vitamin D. Life Sciences 284:119900. https://doi.org/10.1016/j.lfs.2021.119900.

[51] Fidalgo, M., Shekar, P.C., Ang, Y.-S., Fujiwara, Y., Orkin, S.H., Wang, J., 2011. Zfp281 functions as a transcriptional repressor for pluripotency of mouse embryonic stem cells. Stem Cells 29(11):1705–1716. https://doi.org/10.1002/stem.736.

[52] Pieraccioli, M., Nicolai, S., Pitolli, C., Agostini, M., Antonov, A., Malewicz, M., et al., 2018. ZNF281 inhibits neuronal differentiation and is a prognostic marker for neuroblastoma. Proceedings of the National Academy of Sciences of the United States of America 115(28):7356–7361. https://doi.org/10.1073/pnas.1801435115.

[53] Ahrén, B., Winzell, M.S., Pacini, G., 2008. The augmenting effect on insulin secretion by oral versus intravenous glucose is exaggerated by high-fat diet in mice. Journal of Endocrinology 197(1):181–187. https://doi.org/10.1677/JOE-07-0460.

[54] Gupta, D., Jetton, T.L., LaRock, K., Monga, N., Satish, B., Lausier, J., et al., 2017. Temporal characterization of β cell-adaptive and -maladaptive mechanisms during chronic high-fat feeding in C57BL/6NTac mice. Journal of Biological Chemistry 292(30):12449–12459. https://doi.org/10.1074/jbc.M117.781047.

[55] Yamane, S., Harada, N., Inagaki, N., 2016. Mechanisms of fat-induced gastric inhibitory polypeptide/glucose-dependent insulinotropic polypeptide secretion from K cells. Journal of Diabetes Investigation 7(S1):20–26. https://doi.org/10.1111/jdi.12467.

[56] Keller, M.P., Paul, P.K., Rabaglia, M.E., Stapleton, D.S., Schueler, K.L., Broman, A.T., et al., 2016. The transcription factor Nfatc2 regulates β-cell proliferation and genes associated with type 2 diabetes in mouse and human islets. PLoS Genetics 12(12):e1006466. https://doi.org/10.1371/journal.pgen.1006466.

[57] Navarro, G., Xu, W., Jacobson, D.A., Wicksteed, B., Allard, C., Zhang, G., et al., 2016. Extranuclear actions of the androgen receptor enhance glucose-stimulated insulin secretion in the male. Cell Metabolism 23(5):837–851. https://doi.org/10.1016/j.cmet.2016.03.015.

[58] Ravassard, P., Hazhouz, Y., Pechberty, S., Bricout-Neveu, E., Armanet, M., Czernichow, P., et al., 2011. A genetically engineered human pancreatic β cell line exhibiting glucose-inducible insulin secretion. Journal of Clinical Investigation 121:3589–3597.

